

Published in final edited form as:

*Stem Cells*. 2010 November ; 28(11): 1918–1929. doi:10.1002/stem.518.

## Interaction of HIF1 $\alpha$ and Notch Signaling Regulates Medulloblastoma Precursor Proliferation and Fate

Francesca Pistollato<sup>1</sup>, Elena Rampazzo<sup>1</sup>, Luca Persano<sup>1,\*</sup>, Sara Abbadi<sup>1</sup>, Chiara Frasson<sup>1</sup>, Luca Denaro<sup>2</sup>, Domenico D'Avella<sup>2</sup>, David M. Panchision<sup>3</sup>, Alessandro Della Puppa<sup>2</sup>, Renato Scienza<sup>2</sup>, and Giuseppe Basso<sup>1</sup>

<sup>1</sup>SSD Clinical and Experimental Hematology, Department of Paediatrics, University of Padova, Padova, Italy

<sup>2</sup>Department of Neurosurgery, University of Padova, Padova, Italy

<sup>3</sup>Division of Neuroscience and Basic Behavioral Science, National Institute of Mental Health, National Institutes of Health, Bethesda, MD

### Abstract

Medulloblastoma (MDB) is the most common brain malignancy of childhood. It is currently thought that MDB arises from aberrantly functioning stem cells in the cerebellum that fail to maintain proper control of self-renewal. Additionally, it has been reported that MDB cells display higher endogenous Notch signaling activation, known to promote the survival and proliferation of neoplastic neural stem cells and to inhibit their differentiation. While interaction between Hypoxia Inducible Factor-1 $\alpha$  (HIF-1 $\alpha$ ) and Notch signalling is required to maintain normal neural precursors in an undifferentiated state, an interaction has not been identified in MDB. Here we investigate whether hypoxia, through HIF-1 $\alpha$  stabilization, modulates Notch1 signaling in primary MDB-derived cells. Our results indicate that MDB-derived precursor cells require hypoxic conditions for *in vitro* expansion, whereas acute exposure to 20% oxygen induces tumor cell differentiation and death through inhibition of Notch signaling. Importantly, stimulating Notch1 activation with its ligand Dll4 under hypoxic conditions leads to expansion of MDB-derived CD133<sup>+</sup> and nestin<sup>+</sup> precursors, suggesting a regulatory effect on stem cells. In contrast, MDB cells undergo neuronal differentiation when treated with  $\gamma$ -secretase inhibitor, which prevents Notch activation. These results suggest that hypoxia, by maintaining Notch1 in its active form, preserves MDB stem cell viability and expansion.

\*Corresponding author: Persano Luca, PhD, SSD Clinical and Experimental Hematology, Department of Paediatrics, University of Padova, Address: Via Giustiniani 3, 35128 Padova, Italy. Tel: +39 049 8211471; Fax: +39 049 8211462; luca.persano@unipd.it.

Disclaimers: None

### Disclosure of Potential Conflicts of Interest

The authors indicate no potential conflicts of interest.

### Author Contribution Summary:

Francesca Pistollato: Conception and design, Collection and/or assembly of data, Data analysis and interpretation, Manuscript writing, Final approval of manuscript

Elena Rampazzo: Collection and/or assembly of data, Data analysis and interpretation

Luca Persano: Collection and/or assembly of data, Data analysis and interpretation, Manuscript writing, Final approval of manuscript

Sara Abbadi: Collection and/or assembly of data

Chiara Frasson: Collection and/or assembly of data

Luca Denaro: Provision of study material

Domenico D'Avella: Provision of study material

David M. Panchision: Data analysis and interpretation, Manuscript writing

Alessandro Della Puppa: Provision of study material

Renato Scienza: Provision of study material

Giuseppe Basso: Administrative support, Financial support

## Keywords

medulloblastoma; cancer stem cells; hypoxia; Notch1; hypoxia inducible factor-1-alpha

---

## Introduction

Medulloblastoma (MDB) is the most common brain tumor of childhood, accounting for 14.5% of all newly diagnosed cases<sup>1</sup>. They are typically malignant, invasive embryonal tumors of the cerebellum, predominantly displaying neuronal differentiation and an inherent tendency to metastasize via cerebrospinal fluid. It is currently thought that MDB arises from aberrantly functioning stem cells in the cerebellum that fail to maintain proper control of self-renewal<sup>2</sup>. MDB cells display high endogenous activation of Notch<sup>3-6</sup>, a crucial signaling pathway known to promote the survival and proliferation of neoplastic neural stem cells by inhibiting their differentiation<sup>7,8</sup>. Notch signaling is initiated by Delta or Jagged family ligand binding, followed by intramembranous proteolytic cleavage of the Notch receptor by the  $\gamma$ -secretase complex. Inhibitors of this complex slow the growth of Notch-dependent tumors such as MDB and T-cell leukaemia<sup>4,5</sup>, selectively depleting the tumor stem cell fraction<sup>3</sup>. Moreover, brain tumors are often characterized by intra-tumoral hypoxia. Recent literature shows that hypoxia and over-activity of Hypoxia Inducible Factor-1 $\alpha$  (HIF-1 $\alpha$ ) correlate with tumor aggressiveness<sup>9-11</sup> and progression<sup>12</sup>. Hypoxia has a role in normal physiological responses, such as carotid body growth and generation of new neural crest derived glomus cells<sup>13</sup>, angiogenesis<sup>14</sup> and it is implicated in the regulation of crucial signaling pathways, such as bone morphogenetic proteins (BMPs)<sup>15</sup>, Akt/mTOR<sup>16</sup> and Notch<sup>17</sup>. Here, we sought to investigate whether hypoxia and in particular HIF-1 $\alpha$  modulate Notch signalling in primary MDB derived cells. Our results indicate that hypoxia is crucial for MDB stem cell survival and expansion, which is dependent on co-operation of HIF-1 $\alpha$  and Notch1 signaling.

## Materials and Methods

### Isolation and gas-controlled expansion of cells

Written informed consent for the donation of tumor brain tissues was obtained from parents, prior to tissue acquisition, under the auspices of the protocol for the acquisition of human brain tissues obtained from the Ethical Committee board of the University of Padova and Padova Academic Hospital. All tissues were acquired following the tenets of the Declaration of Helsinki. MDB precursors were derived from 13 tumors taken at surgery (see Suppl. Table 1); initial pathological review was followed by secondary neuropathological review to reconfirm diagnosis. We dissociated and cultured cells as previously described<sup>18</sup> (in HAM'SF12/DME, Irvine Scientific, Santa Ana, CA) with additional BIT9500 (10%, serum substitute, Stem Cell Technologies, Vancouver, Canada) and 20 ng/ml epidermal growth factor (EGF, human from R&D Systems, Minneapolis, MN), in an atmosphere of 2% oxygen, 5% carbon dioxide and balanced nitrogen (Ruskinn C300, Ruskinn Technology Ltd, Bridgend, UK) as already described<sup>15</sup>. For continuous expansion, one-half of the medium was replaced every day and cultures were passaged every 7–10 days using TrypLE (Invitrogen, Carlsbad, CA). Cells were not cultured for more than 8 passages *in vitro* in order to avoid long term culture related effects. Normal subventricular zone (SVZ)-derived cells were cultured using the same protocol as that used for their previous extensive characterization<sup>19,20</sup>. In some experiments, MDB-derived cells were supplemented with the immobilized Notch ligand Delta-Like 4 (Dll4, 2 $\mu$ g/ml R&D Systems, Minneapolis, MN) or gamma secretase inhibitor X or IX (DAPT, 10 $\mu$ M, Calbiochem, Nottingham, UK) for 72 hr; both secretase inhibitors elicited analogous Notch1 inhibition.

## Immunohistochemistry

Tumor biopsies were formalin-fixed, paraffin-embedded and cut in 5  $\mu$ m-thick sections. Some sections were used for H&E staining and others for immunohistochemical analyses as previously described<sup>21</sup>. Sections were re-hydrated and antigen retrieval was performed by incubation with either citrate buffer 0.01M pH6 at 95°C for 20' or trypsin at room temperature for 15'. After saturation with 5% BSA, slides were incubated with anti-Notch1 (goat, 1:200, Santa Cruz, Santa Cruz, CA), anti-Hes1 (rabbit 1:500, Chemicon, Billerica, MA), anti-HIF-1 $\alpha$  (mouse, 1:20, BD, Franklin Lakes, NJ; rabbit 1:50, Abcam, Cambridge, MA), anti-nestin (mouse, 1:100, Chemicon, Billerica, MA; rabbit, 1:100, Millipore, Billerica, MA), anti-CD34 (mouse, 1:50, Novocastra, Wetzlar, Germany), anti-CD133 (rabbit, 1:200, Abcam, Cambridge, MA), anti-CAIX (rabbit, 1:1000, Novus Biologicals, Littleton, CO) and anti-Dll4 (rabbit, 1:200, Abcam, Cambridge, MA). After incubation, sections were washed and incubated with species-specific secondary antibodies conjugated to Alexa dyes (Invitrogen, Carlsbad, CA). Tissues were counterstained with DAPI (1:10,000, Sigma-Aldrich, St. Louis, CO) to label cell nuclei. Staining was visualized by epifluorescence (video-confocal, Vico, Nikon, Melville, NY) and images were compiled for figures using Adobe Photoshop and Illustrator (Adobe, San Jose, CA). The specificity of each staining procedure was confirmed by replacing primary antibodies with PBS or matched isotype control.

## Immunocytochemistry

Cells were fixed in 4% paraformaldehyde for 15', rinsed and stored at 4°C prior to analysis. Primary antibody staining was performed for Ki67 (mouse, 1:100, Dako, Glostrup, Denmark), nestin (mouse, 1:200, Chemicon, Billerica, MA), activated caspase-3 (rabbit, 1:2000, Cell Signaling, Danvers, MA), glial fibrillary acidic protein (GFAP, rabbit, 1:1000, Dako, Glostrup, Denmark),  $\beta$ -III-tubulin (Tuj-1, mouse, 1:1000, Covance Princeton, NJ), MAP2 (AP20, mouse, 1:100, Sigma-Aldrich, St. Louis, CO) and p21<sup>cip1</sup> (mouse, 1:800, Calbiochem, Nottingham, UK). After incubation, cells were washed and incubated with species-specific secondary antibodies conjugated to Alexa dyes (Invitrogen, Carlsbad, CA).

To label apoptotic cells a terminal deoxynucleotidyltransferase-mediated dUTP nick end labeling (TUNEL) staining protocol was used using the In Situ Cell Death Detection Kit (Roche Diagnostics, Basel, Switzerland) according to manufacturer's instructions on paraformaldehyde-fixed GBM cell cultures. Cells were counterstained with DAPI (1:10000, Sigma-Aldrich, St. Louis, CO) to identify cell nuclei and count total cell number. Staining was visualized by epifluorescence (Vico, Nikon, Melville, NY) and images were compiled for figures using Adobe Photoshop and Illustrator (Adobe, San Jose, CA).

## Results

### Hypoxia promotes expansion of MDB-derived cells

We previously reported that normal human subventricular zone (SVZ)-derived neural precursor cells undergo enhanced proliferative expansion in lowered, physiologically relevant 5% oxygen compared with standard laboratory conditions of 20% oxygen<sup>20</sup>. Furthermore, primary glioblastoma-derived cells require an even lower, hypoxic 2% oxygen tension for maximal expansion<sup>15, 16</sup>. To determine if MDB-derived neural precursors required the same lowered oxygen tensions for optimal expansion, we performed a similar analysis. We found that 5% and particularly 2% oxygen promoted expansion and long term survival of MDB derived cells (Fig 1A,B). Acute exposure to 20% oxygen for 7 days elicited significant reduction of total cell numbers and, in this condition, MDB cells did not survive for more than two consecutive passages. As previously described, expansion of

normal SVZ-derived neural precursor cells was maximally enhanced by 5% oxygen (Fig 1C), as already reported<sup>20</sup>, but was lower than expansion of MDB.

### Acute exposure to high oxygen tension inhibits proliferation and induces neuronal differentiation in MDB-derived neural precursor cells

In order to determine if the reduced MDB cell expansion in 20% oxygen reflected increased cell death or mitotic arrest, we first analyzed cell growth, expression of the proliferation markers Ki67 and p21<sup>cip1</sup>, and performed cleaved-caspase-3, Annexin-V and TUNEL staining to measure apoptosis levels. We found that MBD derived cells growth was strongly inhibited when cells were cultured at 20% oxygen (Suppl. Fig 1A) and Ki67<sup>+</sup> cells were more abundant in 2% oxygen, indicating higher percentages of actively dividing cells in hypoxic conditions (Fig 2A,F). Conversely, cleaved-caspase3 (Fig 2A,F) and p21<sup>cip1</sup> (Fig 2B,F) were more frequently expressed in MDB cells exposed to 20% oxygen for 48 hr, consistent with the onset of apoptosis and mitotic arrest. Moreover, analyses of Annexin-V/PI and TUNEL staining revealed a modest, albeit not significant, increase in the percentage of apoptotic cells at 20% oxygen, particularly of AnnexinV<sup>+</sup>/PI<sup>+</sup> and TUNEL<sup>+</sup> apoptotic cells (Suppl. Fig 1B,C). These results indicate that an acute exposure to increased oxygen tension inhibits proliferation and slightly promotes apoptosis in MDB derived cells.

In order to evaluate if the observed mitotic arrest resulted in cell differentiation, we analyzed MDB-derived cells for the expression of nestin, an intermediate filament which marks multipotent neural stem cells and the lineage-committed progenitors derived from them, but not differentiated neurons, astrocytes and oligodendrocytes<sup>25</sup>. We also measured expression of glial fibrillary acidic protein (GFAP), which marks both astrocytes and some radial glia<sup>26</sup>,  $\beta$ -III-tubulin, a marker of immature neurons and their committed progenitors<sup>27</sup>, and MAP2, a microtubules associated protein that marks differentiated neurons<sup>28</sup>. In 2% oxygen, MDB-derived cells were mainly nestin<sup>+</sup> precursors with some  $\beta$ -III-tubulin<sup>+</sup> cells, but few if any GFAP<sup>+</sup> or MAP2<sup>+</sup> cells; exposure to 20% oxygen for 48 hr caused a 2-fold increase in the percentage of  $\beta$ -III-tubulin<sup>+</sup> cells, more than 5 fold increase in the percentage of MAP2<sup>+</sup> cells and a decrease in nestin<sup>+</sup> precursors (Fig 2C,D,E,G). To better characterize this response, we dual-labelled cells with nestin/Ki67 or  $\beta$ -III-tubulin/Ki67, which showed that 20% oxygen reduced the percentages of both nestin<sup>+</sup>/Ki67<sup>+</sup> cells and  $\beta$ -III-tubulin<sup>+</sup>/Ki67<sup>+</sup> (Suppl. Fig. 1D,E). There was a concurrent increase in  $\beta$ -III-tubulin<sup>+</sup>/Ki67<sup>-</sup> cells, consistent with a differentiation of neuronal progenitors to post-mitotic neurons (Suppl. Fig. 1E) and the increase of the MAP2<sup>+</sup> cells fraction, as previously shown in Fig 2E,G. Dual labelling with cleaved-caspase3/nestin indicated that, while an increase in apoptotic cells occurred in 20% oxygen compared with 2% oxygen (Fig. 2A,F), only a very small percentage of nestin<sup>+</sup> cells were apoptotic (Suppl. Fig. 1F). This suggests that the apoptotic response to increased oxygen is selective to neuronal progenitors while the anti-proliferative response is common to multiple precursors, possibly including stem cells. Acute exposure to 20% oxygen did not significantly change the low numbers or absence of GFAP<sup>+</sup> (Fig 2D,F) or GFAP<sup>+</sup>/Ki67<sup>+</sup> cells (not shown).

To confirm the observed neuronal commitment of MBD derived cells following acute exposure to high oxygen tension, we analyzed the expression of a series of genes reported to be differentially modulated during neuronal differentiation of cerebellar neural progenitors<sup>29</sup>. In particular, the stem cells related gene Sox2 disclosed a dramatic down-regulation after 48 hr of 20% oxygen exposure (Fig. 2H). On the contrary genes involved in the regulation of the mid-hindbrain regions and the generation of the external granular layer (EGL) of the developing cerebellum (EN1 and Math1), in the formation of granule neuron precursors (Neurod1 and NSCL1), in the migration of more differentiated neuron precursors ( $\beta$ -III-tubulin) and their differentiation to post mitotic neurons (MAP2)<sup>29</sup>, were all up-regulated after 2 days at 20% oxygen (Fig. 2H). Pax6, involved in several stages of

migration of differentiating neurons, did not vary its expression (Fig. 2H). All these data confirm the observed neuronal differentiation of MDB derived cells when exposed at high oxygen tensions and their progressive acquirement of a non cycling neuronal phenotype.

Recent studies have shown that brain tumor progenitors preferentially localize near vasculature but are also present in surrounding hypoxic tissues<sup>30-32</sup>. Vasculature is a source of signals for CNS stem cell self-renewal<sup>33</sup>, but is also a delivery vehicle for oxygen, thereby presenting two potentially antagonistic signals for precursor proliferation<sup>34</sup>. We performed immunohistochemical analyses of MDB tumor tissues to determine if neural precursor numbers co-varied with tumor areas of low or high microvascular density (MVD), measured by CD34 expression<sup>35</sup>. Staining indicated that MDB areas with low MVD had high HIF-1 $\alpha$  expression (Suppl. Fig. 2A,B and Suppl. Table 2), were more enriched in nestin<sup>+</sup> cells and had few  $\beta$ -III-tubulin<sup>+</sup> cells (Suppl. Fig. 2C,D, left panels and Suppl. Table 2), when compared to tumor areas with high MVD (Suppl. Fig. 2C,D, right panels and Suppl. Table 2). GFAP<sup>+</sup> cells were barely detectable in the analyzed MDB samples (not shown).

To verify that HIF-1 $\alpha$  molecule was not just accumulated but also that HIF-1 $\alpha$  signaling was actually activated in MDB tissues, we analyzed the expression of a well known HIF-1 $\alpha$  downstream target gene, carbonic anhydrase IX (CAIX)<sup>36</sup> together with CD34. This confirmed that tumor areas with a low MVD had a higher proportion of CAIX<sup>+</sup> cells (Suppl. Fig. 2E and Suppl. Table 2). These *in vivo* results are consistent with our *in vitro* findings that hypoxia preferentially promotes expansion and survival of MDB-derived precursor cells, while an acute exposure to a higher oxygen tension promotes neuronal differentiation. Consistent with our data, it has been reported that restricted oxygen conditions increase the cancer stem cell fraction and promote acquisition of a stem-like state<sup>30</sup>.

### Acute exposure to high oxygen tension inhibits Notch signaling in MDB derived cells

We then sought to determine the molecular mechanisms by which increased oxygen tension promotes neuronal differentiation of MDB cells. HIF-1 $\alpha$  is rapidly degraded by proteolysis in response to increasing oxygen tension, which explains its actions as a signal transducer of hypoxia<sup>37</sup>; we also found that this rapid degradation occurred in MDB-derived precursors in response to acute 20% oxygen exposure (Fig. 3A). Notch signaling supports the survival, proliferation and prevents differentiation of normal and tumor-derived neural stem cells<sup>4, 5, 8, 38, 39</sup>. Signaling is initiated by the binding of Delta or Jagged ligands to Notch receptors, which leads to intramembranous proteolytic cleavage of the Notch receptor (from a 270 kDa to a 110 kDa protein) by the  $\gamma$ -secretase complex, yielding an activated Notch Intracellular Domain (NICD) that translocates to the nucleus to regulate target gene transcription. We found that Notch signaling was inhibited by acute exposure to 20% oxygen (Fig. 3A), as shown by the decrease of NICD (110 kDa) after 30 min exposure to 20% oxygen. We also found that Delta-like-4 (Dll4), a Notch ligand, was transiently down-regulated within 30 min in 20% oxygen (Fig 3A). Analysis of Notch1-transcriptional activity using a luciferase reporter assay revealed a significant decrease in Notch1 activation when MDB cells were acutely exposed to 20% oxygen (Fig. 3B). We then analyzed Dll4 expression in MDB tissue and found that Dll4 expression was high in tumor areas characterized by low MVD, but was not detectable in presence of high MVD (Suppl. Fig 2F). This is consistent with a previous report showing that Dll4 expression is induced by vascular endothelial growth factor (VEGF)-A and hypoxia<sup>40</sup>.

One Notch1 target gene is the basic-helix-loop-helix transcription factor Hes1, which is known to inhibit neurogenesis and maintain the neural stem cell identity<sup>41</sup>. We found that acute exposure of MDB cells to 20% oxygen caused Hes1 down-regulation along with  $\beta$ -III-

tubulin up-regulation (Fig 3A). This is consistent with a role for downstream Notch target genes in mediating the cell fate responses to changing oxygen tension.

### HIF-1 $\alpha$ is required to maintain Notch1 activation

To investigate whether HIF-1 $\alpha$  is required to maintain Notch1 in its active form, we silenced HIF-1 $\alpha$  with a lentiviral vector bearing a siRNA specific for HIF-1 $\alpha$ <sup>21, 24</sup> (Suppl. Fig 2G). Experiments were performed in 2% oxygen to model conditions in which HIF-1 $\alpha$  is normally active. Silencing of HIF-1 $\alpha$  caused MDB-derived precursors to show morphological differentiation and eventually die by 5–7 days post-transduction (nearly 85% cell death, not shown). In contrast, sham silencing with luciferase siRNA did not induce cell death, thus excluding a non-specific effect of viral infection (not shown). This indicates that HIF-1 $\alpha$  stability may be required to preserve MDB cell viability. During the early stages of morphological differentiation, we found that components of the Notch1 pathway were down-regulated after HIF-1 $\alpha$  silencing; these included total and activated (NICD) Notch, Hes1 and Dll4; sham silencing with luciferase siRNA had little effect on Notch or NICD, but did cause some non-specific down-regulation of Dll4 and Hes1 relative to the unchanged  $\beta$ -actin loading control. In contrast,  $\beta$ -III-tubulin expression increased after silencing HIF-1 $\alpha$ , consistent with increased neuronal differentiation (Fig. 3C). These results provide evidence that HIF-1 $\alpha$  is required to maintain the activation of Notch1 signaling in MDB-derived precursor cells.

### HIF-1 $\alpha$ and Notch1 are co-expressed in MDB precursor cells

Immunohistochemical analysis of MDB tissues indicated that the majority of HIF-1 $\alpha$ <sup>+</sup> cells co-expressed Notch1 and Hes1 (merged images in Fig. 4A,B and Table 1). Moreover, the HIF-1 $\alpha$  downstream target gene CAIX, was found to be expressed in the majority of both HIF-1 $\alpha$ <sup>+</sup> and Notch1<sup>+</sup> MDB cells (Suppl. Fig 3A,B). In accordance to our data, a previous report described that direct interaction between NICD and HIF-1 $\alpha$  occurs in several cell types, such as cortical embryonic stem cells, satellite cells, C2C12 and mouse embryonic teratocarcinoma cell line P19, and HIF-1 $\alpha$  is recruited to Notch-responsive promoters upon Notch activation under hypoxic conditions<sup>17</sup>. Hes1 localization was primarily nuclear and co-localized in the same cells as HIF-1 $\alpha$  (Fig. 4B). The majority of nestin<sup>+</sup> precursor cells resulted to express Notch1 (Fig 4C), and both CD133<sup>+</sup> cells, representative of tumor stem cell fraction, and nestin<sup>+</sup> cells expressed HIF-1 $\alpha$  (Fig. 4D,E) (quantification in Table 1).

### Modulation of Notch1 signaling affects HIF-1 $\alpha$ protein stability and transcriptional activity

Next, we sought to investigate whether exogenous modulation of Notch pathway in MDB derived cells was differentially regulated in 2% oxygen compared to 20% oxygen. We treated cells for 72 hr with immobilized Dll4 (R&D, 2 $\mu$ g/ml) or with DAPT (Calbiochem, 10 $\mu$ M), a  $\gamma$ -secretase inhibitor that prevents Notch cleavage and activation<sup>42–44</sup>. Analyses of total protein confirmed that Notch1 pathway was more strongly activated in 2% oxygen, as shown by an increase of 110 kDa NICD; addition of Dll4 increased this activation as well as Hes1 expression in both oxygen tensions (Fig. 5A). Conversely,  $\beta$ -III-tubulin was slightly down-regulated by Dll4 in 2% oxygen, while Dll4 protein level did not significantly change among conditions (Fig 5A). In contrast, DAPT treated cells underwent inhibition of Notch1 signaling, especially when acutely exposed to 20% oxygen (Fig 5A). In order to verify if DAPT treatment promoted either increased MDB cell differentiation or apoptosis, we tested cleaved caspase3, PARP and p21<sup>cip1</sup> expression; we found increase of p21<sup>cip1</sup> protein level in DAPT treated cells in 2% oxygen, while levels of cleaved caspase3 (not shown) and cleaved PARP did not significantly change (Fig. 5A).

We then analyzed whether HIF-1 $\alpha$  protein stability was altered by Notch1 activation or inhibition. Surprisingly, we found that HIF-1 $\alpha$  protein did not change following Dll4

stimulation, but was reduced in DAPT treated cells (Fig 5A) maintained under hypoxia. Moreover, we found that the level of PHD2, a proline hydroxylase that is a direct sensor of oxygen tension and is responsible for initiating HIF-1 $\alpha$  protein degradation, was higher following DAPT treatment in 2% oxygen (Fig 5A). We previously showed the involvement of the peptidyl prolyl cis/trans isomerase FKBP38 in controlling PHD2 degradation<sup>16</sup>, consistent with previous reports<sup>45, 46</sup>. Indeed, it has been shown that PHD2 protein abundance depends on the membrane-associated localization of FKBP38<sup>46</sup>. Thus, we wanted to determine if a similar PHD2 modulation of HIF-1 $\alpha$  protein levels occurred in MDB cells following DAPT or Dll4 stimulus. We found that Dll4 stimulation in both oxygen tensions promoted up-regulation of FKBP38 (Fig. 5A). In contrast, DAPT promoted a strong reduction of FKBP38 (Fig. 5A). Even though this is not a direct measure of higher PHD2 activation, it indicates that increased PHD2 protein stability is a consequence of Notch inhibition and that this could be mediated by FKBP38.

In order to measure the interaction between HIF-1 $\alpha$  and its cognate consensus sequence (HRE), we used a hypoxia responsive element (HRE)-luciferase reporter assay. We found that 8 hr of Dll4 treatment induced a significant increase of HIF-1 $\alpha$  dependent transcriptional activity in 2% oxygen, in contrast to the effects mediated by DAPT (Fig. 5B). Also, a Notch1-luciferase reporting assay confirmed Dll4-dependent activation in both 2% and 20% oxygen, while DAPT decreased Notch1 signaling more effectively in 2% oxygen (Fig. 5C). This is probably due to the fact that endogenous Notch1 signaling was already inhibited in MDB cells acutely exposed to 20% oxygen (Fig 3B and Fig 5C). Together these results suggest that Notch1 signaling is preferentially activated in MDB-derived cells in hypoxic conditions, and also that Dll4 and DAPT control HIF-1 $\alpha$  mediated transcriptional activity. They also indicate that inhibition of Notch1 signaling by DAPT causes HIF-1 $\alpha$  down-regulation, probably by PHD2 up-regulation.

Furthermore, QRT-PCR analyses revealed that *hes1* transcript was up-regulated by Dll4 only in cells maintained in 2% oxygen (Fig 5D), while *hey1*, another Notch1 downstream target gene involved in the progression of glioblastoma<sup>47</sup>, was more highly expressed after Dll4 treatment, regardless of oxygen tension (not shown). Conversely, *hes1* expression was decreased by DAPT, confirming the effectiveness of DAPT in inhibiting Notch1 pathway activation in 2% and 20% oxygen. Analysis of *dll4*, *hif-1 $\alpha$*  and *phd2* gene expression did not show significant differences among conditions (not shown), suggesting that the observed modulations in protein expression levels do not necessarily reflect transcriptional changes.

### Notch1 signaling modulation affects MDB cell phenotype depending on hypoxia

We and others previously provided evidence that hypoxia either instructs or selects for a more primitive phenotype of tumor cell<sup>10, 11, 15</sup> and that HIF-1 $\alpha$  is an important factor in promoting this cell state<sup>15, 17</sup>. We tested whether the interaction between Notch signaling and HIF-1 $\alpha$  regulated the relative abundance of MDB-derived precursor cells compared with more differentiated cell types. We tested this by activating Notch1 signaling with Dll4 and found an increase in CD133<sup>+</sup>, marking stem cells, and nestin<sup>+</sup> cells (i.e. nestin<sup>+</sup>/ $\beta$ -III-tubulin<sup>-</sup>) in 2% oxygen but not 20% oxygen within 72 hr of treatment (Fig 6A,B,F). Interestingly, this treatment led to a decrease in  $\beta$ -III-tubulin<sup>+</sup> cells (i.e. nestin<sup>-</sup>/ $\beta$ -III-tubulin<sup>+</sup>) in 20% oxygen but not 2% oxygen (Fig 6B,F). Another cell surface marker, CD15, is used analogously to CD133 as a stem cell marker for normal and MDB-derived cells in mouse models<sup>18, 48, 49</sup>, but we did not see any change in the percentage of CD15<sup>+</sup> cells following Dll4 or DAPT treatments (not shown). Interestingly, Dll4 treatment led to a decrease in mitotically active cells (measured by Ki67 expression) in both oxygen tensions relative to their control counterparts (Fig 6D), suggesting that Notch signalling promotes quiescence that is characteristic of slowly dividing stem cells<sup>8, 50</sup>. This effect was much stronger during acute exposure to 20% oxygen, where Dll4 treatment led to a substantial

reduction in both Ki67 expression and total cell number (Fig. 6D,E,F). This is consistent with the anti-proliferative effect of Dll4 previously described for other cell types<sup>51,52</sup>.

We found that inhibition of Notch signalling with DAPT, despite also having an indirect inhibitory effect on HIF-1 $\alpha$  (Fig 5A,B), did not reduce CD133<sup>+</sup> cell numbers within 72 hr (Fig. 6A); however, it did reduce numbers of nestin<sup>+</sup> cells and increase numbers of  $\beta$ -III-tubulin<sup>+</sup> cells under both 2% and 20% oxygen tensions (Fig 6B,C,F). Mitotically active cell numbers, as measured by Ki67 staining, were also reduced by DAPT (Fig. 6D), while total cell numbers were slightly but not significantly reduced following DAPT stimulus compared to control group at 2% oxygen (Fig. 6E). The observed decrease of total cells number is not related to increased cell death by DAPT, as shown by analysis of cleaved PARP (Fig. 5A), but rather to increased cell differentiation, as shown by higher p21<sup>cip1</sup> expression (Fig. 5A). MDB cells treated with DAPT and acutely exposed to high oxygen tension did not undergo further decrease of Ki67 expression and of total cells number compared to 20% oxygen control group (Fig. 6D,E). In total, our results suggest that Notch1 activation, by promoting the un-differentiated cellular state, makes MDB precursor cells more sensitive to the effects of changing oxygen tensions.

## Discussion

There is increasing evidence that MDB, like many other cancer types, originates from and is maintained by aberrantly functioning stem cells in the cerebellum that fail to maintain proper control of self-renewal<sup>2</sup>. Since an important feature of stem cells is their quiescence relative to their more active daughter progenitors<sup>50</sup>, the failure to adequately target slowly dividing “cancer stem cells” during clinical treatment may be responsible for cases of tumor recurrence. Notch signalling has been implicated in regulating MDB-derived precursors with stem cell properties<sup>3–6</sup> and is found to promote the survival and proliferation and inhibit differentiation of tumor-derived precursors<sup>7,8</sup>. Our results show that Notch signalling requires hypoxia to maintain MDB-derived precursors in an undifferentiated state and suggest that Notch signalling in turn sensitizes these precursors to changes in oxygen tension. Furthermore, we show that these responses are mediated by a reciprocal interaction between components of the Notch signalling pathway and HIF-1 $\alpha$ , a canonical effector of oxygen response signalling.

While measurements of oxygen in non-neoplastic human brain show a mean oxygen tension varying from 3.2% ( $23.8 \pm 8.1$  mmHg) at 22–27 mm below the dura to 4.4% ( $33.3 \pm 13.3$  mm Hg) at 7–12 mm below the dura<sup>53</sup>, levels below these are a consistent feature of brain tumors<sup>54</sup>. Several reports showed a decrease in oxygen tension in human brain tumors, including reductions of flow and oxygen utilization<sup>55,56</sup>. Even though direct measurements of oxygen tension specifically in MDB tissues have not been directly performed, it is reasonable to hypothesize that MDB cells reside within a hypoxic niche. According to this hypothesis, it has been reported that intracerebral tumors and MDB are characterized by a higher percentage of hypoxic cells, compared to other neoplasms and for this reason higher doses of radiation therapy are required to get equivalent cell killing<sup>57</sup>. Moreover, both hypoxic conditions and HIF-1 $\alpha$  over-activation correlate with tumor aggressiveness<sup>9–12, 15</sup>. Our previous results showed that HIF-1 $\alpha$  is an important mediator of this response, in part through its modulation of key intracellular pathways that regulate precursor cell proliferation and fate, such as BMP and Akt/mTOR signalling in glioblastoma<sup>15,16</sup>. Here we show that, in MDB, hypoxia and HIF-1 $\alpha$  also regulate Notch signalling. This interaction was previously identified in fetal mouse neural precursors<sup>17</sup>, but our work provides the first characterization of this interaction and its novel reciprocal features in MDB-derived precursors.



We show that MDB derived cells, which can be expanded successfully *in vitro* only when cultured under hypoxic condition, undergo differentiation and eventually cell death when acutely exposed to high oxygen tension. This occurs in part through Notch1 signaling inhibition. We found that Notch signaling is activated by hypoxia and its transducer HIF-1 $\alpha$ , while it is down-regulated following acute exposure to high oxygen or HIF-1 $\alpha$  silencing. Our *in situ* histological analysis shows that Notch1 signaling is higher within tumor areas with low MVD, where MDB cell precursors are more abundant. Recent studies have shown that within brain tumors, cancer stem cells preferentially reside near both vasculature and in surrounding necrotic and/or less vascularized (i.e. hypoxic) tissues<sup>30–32</sup>. Consistent with our data, it has been reported that restricted oxygen conditions increase the cancer stem cell fraction and promote acquisition of a stem-like cell features<sup>30</sup>. While the preferential association of cancer stem cells with both vascularized and non-vascularized regions may seem paradoxical, we have hypothesized that vascular regions may actually promote both stem cell properties and quiescence because of the combination of vascular niche factors and higher oxygenation, while specifically restricting oxygen may activate stem cells to re-enter the cell cycle and undergo self-renewal and/or transit-amplifying divisions<sup>34</sup>. In our culture conditions of low oxygen tension (2% O<sub>2</sub>) CD133<sup>+</sup> cells derived from MDB tissues disclosed clonogenic potential in respect to CD133<sup>-</sup> MDB cells (Suppl. Fig. 4). CD133<sup>+</sup> cells have been isolated from different types of brain tumors including MDB and were shown to form aggressive tumors in the brain of mice when injected at low numbers<sup>58, 59</sup>. The utility of CD133 in the isolation of cells with tumor initiating properties has been confirmed by several research groups<sup>60, 61</sup>, but it is unclear whether this marker really identifies tumor initiating cells or a subset of cells that can resist the immune system in partially immunodeficient mice strains. Recent works reported that the CD133<sup>-</sup> population from GBM tumors is able to produce orthotopic tumors even if with a lower efficiency<sup>62, 63</sup>. However, at this time no cell marker is considered absolute in identifying brain tumor stem cells<sup>64</sup>. Thus, since we did not evaluate the *in vivo* tumorigenicity of MDB derived CD133<sup>+</sup> cells maintained in hypoxic culture conditions, our hypotheses on the diverging role of the vascular and hypoxic stem cell niche remain speculative.

We found that HIF-1 $\alpha$  and Notch signaling occur in a high proportion of nestin<sup>+</sup> MDB precursors, while inhibition of Notch signaling by DAPT promotes neuronal differentiation. The increase in CD133<sup>+</sup> cell numbers by Notch activation in 2% oxygen suggests that hypoxia is required for MDB stem cell maintenance, consistent with our previous report on glioblastoma<sup>16</sup>. Another potential link between HIF-1 $\alpha$  and Notch signaling is found in recent work showing that Factor Inhibiting HIF-1 (FIH-1) regulates asparagine hydroxylation of both HIF- $\alpha$  and Notch1-3<sup>65</sup>. Additionally, in mouse embryonic stem cells the hypoxia-induced increase of HIF-1 $\alpha$  promotes Notch-1 activation via Wnt-1 signaling<sup>66</sup>. Thus, there appear to be several levels of shared molecular regulatory mechanisms between Notch and HIF1 $\alpha$ .

*Hes1*, a Notch1 target gene, is one of the gene mammalian homologues of *Drosophila* *Hairy* and *Enhancer of split*, which encode basic helix-loop-helix (bHLH) transcriptional repressors. In the developing central nervous system, *hes* genes are highly expressed in neural stem cells and their inactivation leads to accelerated neurogenesis and premature depletion of neural stem cells<sup>41</sup>. We found that Dll4 treatment increased *Hes1* protein levels in both 2% and 20% oxygen, while *hes1* transcript was upregulated by Dll4 only under hypoxia, which is consistent with HIF-1 $\alpha$ -dependent Notch1 activation and consequentially maintenance of MDB stem cells. Additionally, DAPT treated cells undergo a decrease of HIF-1 $\alpha$  level, phenomenon correlated to PHD2 stabilization. As a consequence, DAPT treated cells undergo neuronal differentiation, as shown by higher proportion of  $\beta$ -III-tubulin<sup>+</sup> cells.

## Conclusion

Our results suggest that two components of the tumor microenvironment, cell-to-cell signaling through Notch and oxygen sensing through HIF-1 $\alpha$ , regulate precursor proliferation and fate and may exert specific control on stem cell quiescence. While definitive evidence of this requires prospective isolation of these cells and testing of tumor reconstitution *in vivo*, our results provide mechanistic insight into how stem cell niche signals may be utilized by cancer stem cells to promote tumor aggression. This in turn can potentially be exploited to selectively target the cells that initiate and maintain MDB, thereby increasing the success rate of treatment.

## Supplementary Material

Refer to Web version on PubMed Central for supplementary material.

## Acknowledgments

Support: This work was supported by funds from the Italian Association for the Fight against Neuroblastoma (Pensiero Project) and the Italian Association AIRC (Interregional paediatric project grant).

We thank Dr. Pier Giorgio Modena, from CRO, Aviano, Italy, for providing MDB-derived cells and Prof. Felice Giangaspero, from University of “La Sapienza” Rome, for providing a quote of MDB histological samples. We are grateful to Dr. Stefano Indraccolo for lentiviral vectors production and thank Dr. Andrea Zangrando for his help with images management. This research was supported by funds from the Italian Association for the Fight against Neuroblastoma (Pensiero Project) and the Italian Association AIRC (Interregional paediatric project grant).

## References

- Partap S, Curran EK, Propp JM, Le GM, Sainani KL, Fisher PG. Medulloblastoma incidence has not changed over time: a CBTRUS study. *J Pediatr Hematol Oncol*. Dec; 2009 31(12):970–971. [PubMed: 19887963]
- Fan X, Eberhart CG. Medulloblastoma stem cells. *J Clin Oncol*. Jun 10; 2008 26(17):2821–2827. [PubMed: 18539960]
- Fan X, Matsui W, Khaki L, et al. Notch pathway inhibition depletes stem-like cells and blocks engraftment in embryonal brain tumors. *Cancer Res*. Aug 1; 2006 66(15):7445–7452. [PubMed: 16885340]
- Fan X, Mikolaenko I, Elhassan I, et al. Notch1 and notch2 have opposite effects on embryonal brain tumor growth. *Cancer Res*. Nov 1; 2004 64(21):7787–7793. [PubMed: 15520184]
- Hallahan AR, Pritchard JJ, Hansen S, et al. The SmoA1 mouse model reveals that notch signaling is critical for the growth and survival of sonic hedgehog-induced medulloblastomas. *Cancer Res*. Nov 1; 2004 64(21):7794–7800. [PubMed: 15520185]
- Raffel C, Jenkins RB, Frederick L, et al. Sporadic medulloblastomas contain PTCH mutations. *Cancer Res*. Mar 1; 1997 57(5):842–845. [PubMed: 9041183]
- Reya T, Morrison SJ, Clarke MF, Weissman IL. Stem cells, cancer, and cancer stem cells. *Nature*. Nov 1; 2001 414(6859):105–111. [PubMed: 11689955]
- Solecki DJ, Liu XL, Tomoda T, Fang Y, Hatten ME. Activated Notch2 signaling inhibits differentiation of cerebellar granule neuron precursors by maintaining proliferation. *Neuron*. Aug 30; 2001 31(4):557–568. [PubMed: 11545715]
- Azuma Y, Chou SC, Lininger RA, Murphy BJ, Varia MA, Raleigh JA. Hypoxia and differentiation in squamous cell carcinomas of the uterine cervix: pimonidazole and involucrin. *Clin Cancer Res*. Oct 15; 2003 9(13):4944–4952. [PubMed: 14581369]
- Helczynska K, Kronblad A, Jogi A, et al. Hypoxia promotes a dedifferentiated phenotype in ductal breast carcinoma in situ. *Cancer Res*. Apr 1; 2003 63(7):1441–1444. [PubMed: 12670886]

11. Jogi A, Ora I, Nilsson H, et al. Hypoxia alters gene expression in human neuroblastoma cells toward an immature and neural crest-like phenotype. *Proc Natl Acad Sci U S A*. May 14; 2002 99(10):7021–7026. [PubMed: 12011461]
12. Smith K, Gunaratnam L, Morley M, Franovic A, Mekhail K, Lee S. Silencing of epidermal growth factor receptor suppresses hypoxia-inducible factor-2-driven VHL<sup>-/-</sup> renal cancer. *Cancer Res*. Jun 15; 2005 65(12):5221–5230. [PubMed: 15958567]
13. Pardal R, Ortega-Saenz P, Duran R, Lopez-Barneo J. Glia-like stem cells sustain physiologic neurogenesis in the adult mammalian carotid body. *Cell*. Oct 19; 2007 131(2):364–377. [PubMed: 17956736]
14. Wong ET, Brem S. Antiangiogenesis treatment for glioblastoma multiforme: challenges and opportunities. *J Natl Compr Canc Netw*. May; 2008 6(5):515–522. [PubMed: 18492463]
15. Pistollato F, Chen HL, Rood BR, et al. Hypoxia and HIF1alpha repress the differentiative effects of BMPs in high-grade glioma. *Stem Cells*. Jan; 2009 27(1):7–17. [PubMed: 18832593]
16. Pistollato F, Rampazzo E, Abbadi S, et al. Molecular mechanisms of HIF-1alpha modulation induced by oxygen tension and BMP2 in glioblastoma derived cells. *PLoS One*. 2009; 4(7):e6206. [PubMed: 19587783]
17. Gustafsson MV, Zheng X, Pereira T, et al. Hypoxia requires notch signaling to maintain the undifferentiated cell state. *Dev Cell*. Nov; 2005 9(5):617–628. [PubMed: 16256737]
18. Panchision DM, Chen HL, Pistollato F, Papini D, Ni HT, Hawley TS. Optimized flow cytometric analysis of central nervous system tissue reveals novel functional relationships among cells expressing CD133, CD15, and CD24. *Stem Cells*. Jun; 2007 25(6):1560–1570. [PubMed: 17332513]
19. Schwartz PH, Bryant PJ, Fuja TJ, Su H, O'Dowd DK, Klassen H. Isolation and characterization of neural progenitor cells from post-mortem human cortex. *J Neurosci Res*. Dec 15; 2003 74(6):838–851. [PubMed: 14648588]
20. Pistollato F, Chen HL, Schwartz PH, Basso G, Panchision DM. Oxygen tension controls the expansion of human CNS precursors and the generation of astrocytes and oligodendrocytes. *Mol Cell Neurosci*. Jul; 2007 35(3):424–435. [PubMed: 17498968]
21. Favaro E, Nardo G, Persano L, et al. Hypoxia inducible factor-1alpha inactivation unveils a link between tumor cell metabolism and hypoxia-induced cell death. *Am J Pathol*. Oct; 2008 173(4):1186–1201. [PubMed: 18772337]
22. Arsham AM, Plas DR, Thompson CB, Simon MC. Phosphatidylinositol 3-kinase/Akt signaling is neither required for hypoxic stabilization of HIF-1 alpha nor sufficient for HIF-1-dependent target gene transcription. *J Biol Chem*. Apr 26; 2002 277(17):15162–15170. [PubMed: 11859074]
23. Razorenova OV, Ivanov AV, Budanov AV, Chumakov PM. Virus-based reporter systems for monitoring transcriptional activity of hypoxia-inducible factor 1. *Gene*. Apr 25; 2005 350(1):89–98. [PubMed: 15794924]
24. Indraccolo S, Roni V, Zamarchi R, et al. Expression from cell type-specific enhancer-modified retroviral vectors after transduction: influence of marker gene stability. *Gene*. Jan 23; 2002 283(1–2):199–208. [PubMed: 11867226]
25. Tohyama T, Lee VM, Rorke LB, Marvin M, McKay RD, Trojanowski JQ. Nestin expression in embryonic human neuroepithelium and in human neuroepithelial tumor cells. *Lab Invest*. Mar; 1992 66(3):303–313. [PubMed: 1538585]
26. Casper KB, McCarthy KD. GFAP-positive progenitor cells produce neurons and oligodendrocytes throughout the CNS. *Mol Cell Neurosci*. Apr; 2006 31(4):676–684. [PubMed: 16458536]
27. Memberg SP, Hall AK. Dividing neuron precursors express neuron-specific tubulin. *J Neurobiol*. May; 1995 27(1):26–43. [PubMed: 7643073]
28. Dehmelt L, Halpain S. The MAP2/Tau family of microtubule-associated proteins. *Genome Biol*. 2005; 6(1):204. [PubMed: 15642108]
29. Wang VY, Zoghbi HY. Genetic regulation of cerebellar development. *Nat Rev Neurosci*. Jul; 2001 2(7):484–491. [PubMed: 11433373]
30. Heddleston JM, Li Z, McLendon RE, Hjelmeland AB, Rich JN. The hypoxic microenvironment maintains glioblastoma stem cells and promotes reprogramming towards a cancer stem cell phenotype. *Cell Cycle*. Oct 15; 2009 8(20):3274–3284. [PubMed: 19770585]

31. Calabrese C, Poppleton H, Kocak M, et al. A perivascular niche for brain tumor stem cells. *Cancer Cell*. Jan; 2007 11(1):69–82. [PubMed: 17222791]
32. Gilbertson RJ, Rich JN. Making a tumour's bed: glioblastoma stem cells and the vascular niche. *Nat Rev Cancer*. Oct; 2007 7(10):733–736. [PubMed: 17882276]
33. Shen Q, Wang Y, Kokovay E, et al. Adult SVZ stem cells lie in a vascular niche: a quantitative analysis of niche cell-cell interactions. *Cell Stem Cell*. Sep 11; 2008 3(3):289–300. [PubMed: 18786416]
34. Panchision DM. The role of oxygen in regulating neural stem cells in development and disease. *J Cell Physiol*. Sep; 2009 220(3):562–568. [PubMed: 19441077]
35. Netto GC, Bleil CB, Hilbig A, Coutinho LM. Immunohistochemical evaluation of the microvascular density through the expression of TGF-beta (CD 105/endoglin) and CD 34 receptors and expression of the vascular endothelial growth factor (VEGF) in oligodendrogliomas. *Neuropathology*. Feb; 2008 28(1):17–23. [PubMed: 18181830]
36. Liao SY, Lerman MI, Stanbridge EJ. Expression of transmembrane carbonic anhydrases, CAIX and CAXII, in human development. *BMC Dev Biol*. 2009; 9:22. [PubMed: 19291313]
37. Bruick RK, McKnight SL. A conserved family of prolyl-4-hydroxylases that modify HIF. *Science*. Nov 9; 2001 294(5545):1337–1340. [PubMed: 11598268]
38. Gaiano N, Fishell G. The role of notch in promoting glial and neural stem cell fates. *Annu Rev Neurosci*. 2002; 25:471–490. [PubMed: 12052917]
39. Weng AP, Ferrando AA, Lee W, et al. Activating mutations of NOTCH1 in human T cell acute lymphoblastic leukemia. *Science*. Oct 8; 2004 306(5694):269–271. [PubMed: 15472075]
40. Williams CK, Li JL, Murga M, Harris AL, Tosato G. Up-regulation of the Notch ligand Delta-like 4 inhibits VEGF-induced endothelial cell function. *Blood*. Feb 1; 2006 107(3):931–939. [PubMed: 16219802]
41. Kageyama R, Ohtsuka T, Kobayashi T. Roles of Hes genes in neural development. *Dev Growth Differ*. Jun; 2008 50 (Suppl 1):S97–103. [PubMed: 18430159]
42. Ikeuchi T, Sisodia SS. Cell-free generation of the notch1 intracellular domain (NICD) and APP-CTF $\gamma$ : evidence for distinct intramembranous “gamma-secretase” activities. *Neuromolecular Med*. 2002; 1(1):43–54. [PubMed: 12025815]
43. Martys-Zage JL, Kim SH, Berechid B, et al. Requirement for presenilin 1 in facilitating lagged 2-mediated endoproteolysis and signaling of notch 1. *J Mol Neurosci*. Dec; 2000 15(3):189–204. [PubMed: 11303783]
44. Schroeter EH, Ilagan MX, Brunkan AL, et al. A presenilin dimer at the core of the gamma-secretase enzyme: insights from parallel analysis of Notch 1 and APP proteolysis. *Proc Natl Acad Sci U S A*. Oct 28; 2003 100(22):13075–13080. [PubMed: 14566063]
45. Barth S, Nesper J, Hasgall PA, et al. The peptidyl prolyl cis/trans isomerase FKBP38 determines hypoxia-inducible transcription factor prolyl-4-hydroxylase PHD2 protein stability. *Mol Cell Biol*. May; 2007 27(10):3758–3768. [PubMed: 17353276]
46. Barth S, Edlich F, Berchner-Pfannschmidt U, et al. Hypoxia-inducible factor prolyl-4-hydroxylase PHD2 protein abundance depends on integral membrane anchoring of FKBP38. *J Biol Chem*. Aug 21; 2009 284(34):23046–23058. [PubMed: 19546213]
47. Hulleman E, Quarto M, Vernell R, et al. A role for the transcription factor HEY1 in glioblastoma. *J Cell Mol Med*. Jan; 2009 13(1):136–146. [PubMed: 18363832]
48. Read TA, Fogarty MP, Markant SL, et al. Identification of CD15 as a marker for tumor-propagating cells in a mouse model of medulloblastoma. *Cancer Cell*. Feb 3; 2009 15(2):135–147. [PubMed: 19185848]
49. Ward RJ, Lee L, Graham K, et al. Multipotent CD15+ cancer stem cells in patched-1-deficient mouse medulloblastoma. *Cancer Res*. Jun 1; 2009 69(11):4682–4690. [PubMed: 19487286]
50. Alvarez-Buylla A, Lois C. Neuronal stem cells in the brain of adult vertebrates. *Stem Cells*. May; 1995 13(3):263–272. [PubMed: 7613493]
51. Chadwick N, Fennessy C, Nostro MC, Baron M, Brady G, Buckle AM. Notch induces cell cycle arrest and apoptosis in human erythroleukaemic TF-1 cells. *Blood Cells Mol Dis*. Nov-Dec; 2008 41(3):270–277. [PubMed: 18693120]

52. Chadwick N, Nostro MC, Baron M, Mottram R, Brady G, Buckle AM. Notch signaling induces apoptosis in primary human CD34+ hematopoietic progenitor cells. *Stem Cells*. Jan; 2007 25(1): 203–210. [PubMed: 16973835]
53. Dings J, Jager A, Meixensberger J, Roosen K. Brain tissue pO<sub>2</sub> and outcome after severe head injury. *Neurol Res*. 1998; 20 (Suppl 1):S71–75. [PubMed: 9584929]
54. Ljungkvist AS, Bussink J, Kaanders JH, van der Kogel AJ. Dynamics of tumor hypoxia measured with bioreductive hypoxic cell markers. *Radiat Res*. Feb; 2007 167(2):127–145. [PubMed: 17390721]
55. Ito M, Lammertsma AA, Wise RJ, et al. Measurement of regional cerebral blood flow and oxygen utilisation in patients with cerebral tumours using <sup>15</sup>O and positron emission tomography: analytical techniques and preliminary results. *Neuroradiology*. 1982; 23(2):63–74. [PubMed: 6979003]
56. McKenzie CG, Lenzi GL, Jones T, Moss S. Radioactive oxygen <sup>15</sup>O studies in cerebral neoplasms. *J R Soc Med*. Jun; 1978 71(6):417–425. [PubMed: 702481]
57. Leith JT, Cook S, Chougule P, et al. Intrinsic and extrinsic characteristics of human tumors relevant to radiosurgery: comparative cellular radiosensitivity and hypoxic percentages. *Acta Neurochir Suppl*. 1994; 62:18–27. [PubMed: 7717130]
58. Hemmati HD, Nakano I, Lazareff JA, et al. Cancerous stem cells can arise from pediatric brain tumors. *Proc Natl Acad Sci U S A*. Dec 9; 2003 100(25):15178–15183. [PubMed: 14645703]
59. Singh SK, Hawkins C, Clarke ID, et al. Identification of human brain tumour initiating cells. *Nature*. Nov 18; 2004 432(7015):396–401. [PubMed: 15549107]
60. Bao S, Wu Q, McLendon RE, et al. Glioma stem cells promote radioresistance by preferential activation of the DNA damage response. *Nature*. Dec 7; 2006 444(7120):756–760. [PubMed: 17051156]
61. Piccirillo SG, Reynolds BA, Zanetti N, et al. Bone morphogenetic proteins inhibit the tumorigenic potential of human brain tumour-initiating cells. *Nature*. Dec 7; 2006 444(7120):761–765. [PubMed: 17151667]
62. Beier D, Hau P, Proescholdt M, et al. CD133(+) and CD133(-) glioblastoma-derived cancer stem cells show differential growth characteristics and molecular profiles. *Cancer Res*. May 1; 2007 67(9):4010–4015. [PubMed: 17483311]
63. Sakariassen PO, Prestegarden L, Wang J, et al. Angiogenesis-independent tumor growth mediated by stem-like cancer cells. *Proc Natl Acad Sci U S A*. Oct 31; 2006 103(44):16466–16471. [PubMed: 17056721]
64. Hadjipanayis CG, Van Meir EG. Brain cancer propagating cells: biology, genetics and targeted therapies. *Trends Mol Med*. Nov; 2009 15(11):519–530. [PubMed: 19889578]
65. Wilkins SE, Hyvarinen J, Chicher J, et al. Differences in hydroxylation and binding of Notch and HIF-1 $\alpha$  demonstrate substrate selectivity for factor inhibiting HIF-1 (FIH-1). *Int J Biochem Cell Biol*. Jul; 2009 41(7):1563–1571. [PubMed: 19401150]
66. Lee SH, Kim MH, Han HJ. Arachidonic acid potentiates hypoxia-induced VEGF expression in mouse embryonic stem cells: involvement of Notch, Wnt, and HIF-1 $\alpha$ . *Am J Physiol Cell Physiol*. Jul; 2009 297(1):C207–216. [PubMed: 19339510]

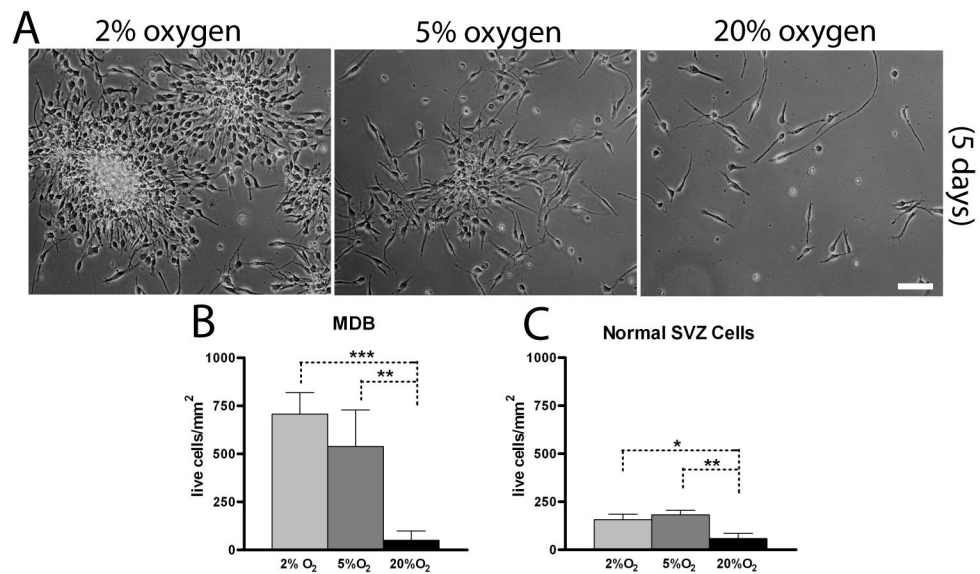


**Figure 1. 2% oxygen preserves viability and proliferation of MDB derived cells**

(A) representative pictures of HuTu33 cells expanded at 2%, 5% or 20% oxygen for 7 days. (B,C) Total cell number counts (by trypan blue exclusion) of MDB (B) and SVZ cells (HuSC30 and HuSC23) (C) cultured for 7 days. For (B), mean of 5 different MDB  $\pm$  S.E.M.,  $n = 2$  for each tumor; for (C), mean of 2 different normal SVZ cells cultures  $\pm$  S.E.M.,  $n = 4$  for each cell culture. 10X pictures, bar = 100  $\mu$ m. \* $p < 0.05$ , \*\* $p < 0.01$ , \*\*\* $p < 0.001$ .

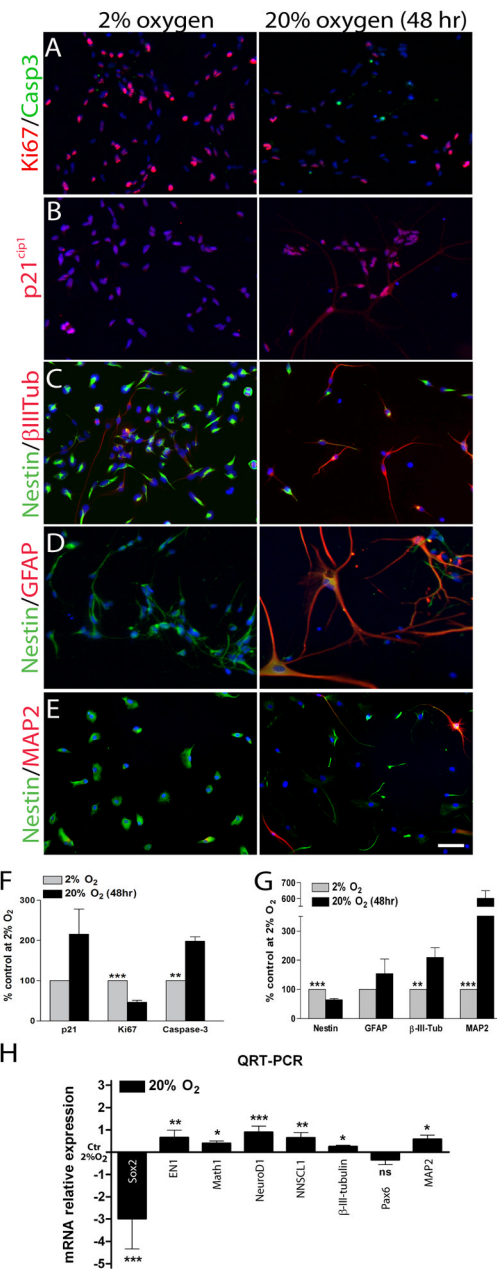


**Figure 2. Acute exposure to high oxygen tension promotes neuronal differentiation, mitotic arrest and eventually cell death in MDB derived cells** (A) Representative immunocytochemical images (HuTu33) of (A) Ki67 (red)/cleaved-Caspase3 (green), (B) p21<sup>cip1</sup> (red), (C) nestin (green)/β-III-tubulin (red), (D) nestin (green)/GFAP (red) and (E) nestin (green)/MAP2 (red) staining of MDB cells expanded for 2 days at either 2% or 20% oxygen. Quantifications in (F,G); for all graphs, mean of 5 different MDB ± S.E.M., n = 3 for each tumor. (H) QRT-PCR analyses of *Sox2*, *EN1*, *Math1*, *NeuroD1*, *NSCL1*, *β-III-tubulin*, *Pax6* and *MAP2*, normalized to *gusb* and then calibrated to 2% oxygen control. Mean ± S.E.M of 4 different MDB. \*p < 0.05, \*\*p < 0.01, \*\*\*p < 0.001, ns: not significant.

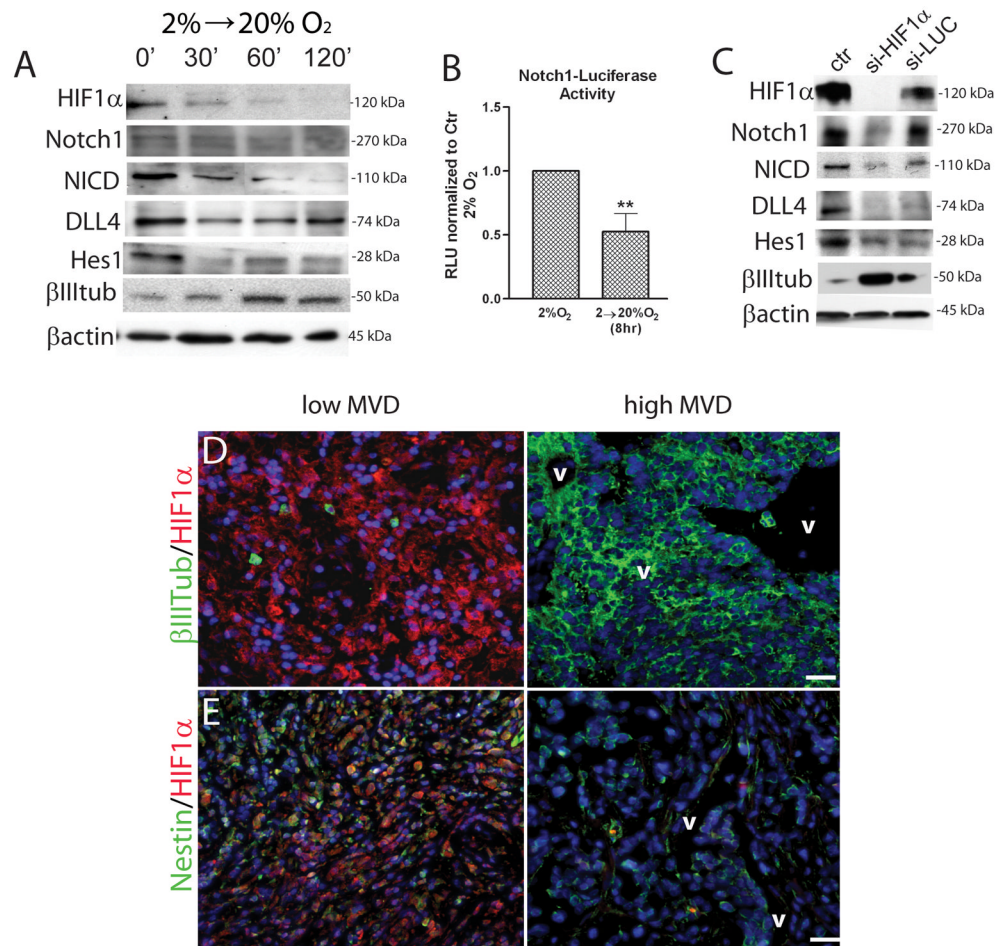


**Figure 3. Acute exposure to high oxygen tension promotes Notch1 pathway inhibition and HIF-1α is required to maintain Notch1 signaling activated**  
 (A) Representative western blot analyses of HIF-1α, Notch1, NICD, DLL4, Hes1, β-III-tubulin and β-actin of MDB cells acutely exposed to 20% oxygen for 30, 60 or 120 minutes. (B) Notch1-Luciferase transfected MDB cells, have been either left at 2% oxygen or acutely exposed to 20% oxygen for 8 hrs. The graph reports mean of 3 different MDB. (C) Representative western blot analyses of cells that had been transduced with a siHIF-1α/EGFP or si-LUC/EGFP bearing vectors. (D,E) Representative immunohistochemical images of (D) HIF-1α (red)/β-III-tubulin (green), (E) HIF-1α (red)/nestin (green) staining of MDB tissues. See quantification in Suppl. Table 2. Magnification 10X, bar = 100 μm. \*p < 0.05, \*\*p < 0.01, \*\*\*p < 0.001. RLU, relative light units; v, vessels; MVD, microvessel density.



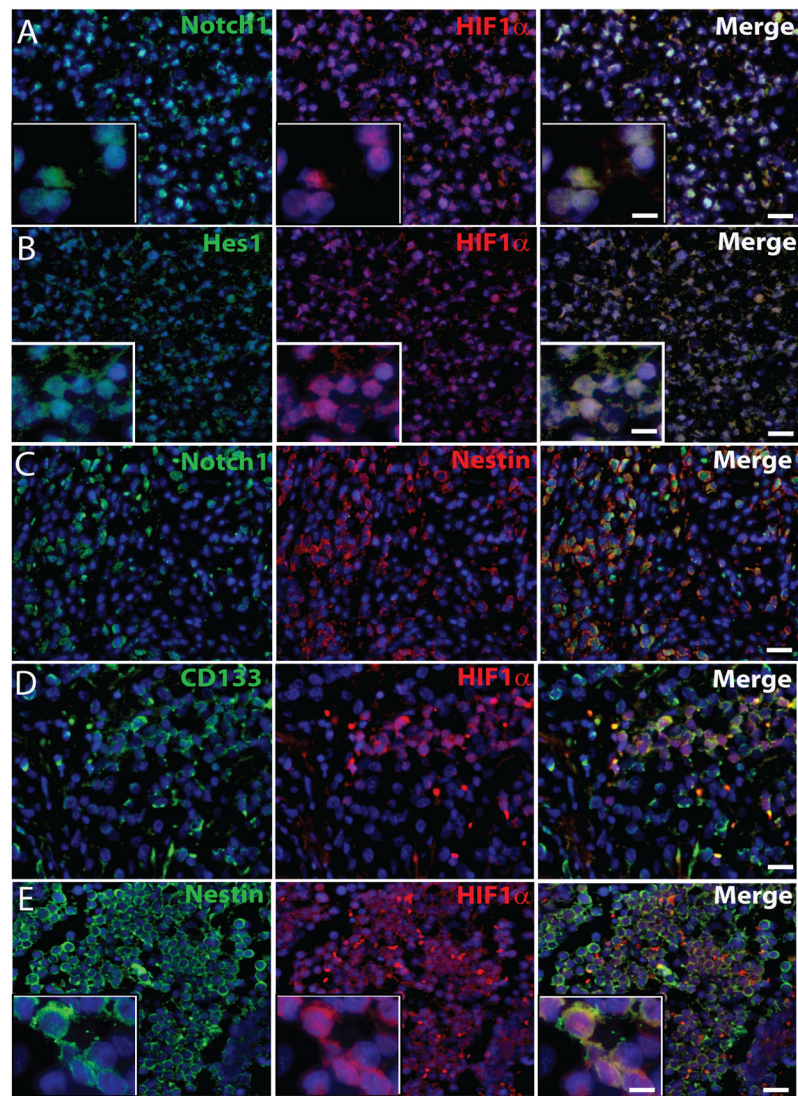


**Figure 4. Notch1, Hes1 and HIF-1 $\alpha$  are co-expressed in nestin<sup>+</sup> and CD133<sup>+</sup> MDDB cells *in vivo***  
 Representative immunohistochemical images of (A) HIF-1 $\alpha$  (red)/Notch1 (green), (B) HIF-1 $\alpha$  (red)/Hes1 (green), (C) nestin (red)/Notch1 (green), (D) HIF-1 $\alpha$  (red)/CD133 (green) and (E) HIF-1 $\alpha$  (red)/nestin (green) staining of MDDB tissues. Insets in panel A, B show nuclear localization of Notch1 (left, A), HIF-1 $\alpha$  (middle, A, B and E), and Hes1 (left, B) and cytoplasmic localization of nestin (left, E). 10X pictures, bar = 100  $\mu$ m (for A,B,C,D,E), 60X insets, bar = 20  $\mu$ m (in A,B merge). See quantification in Table 1.

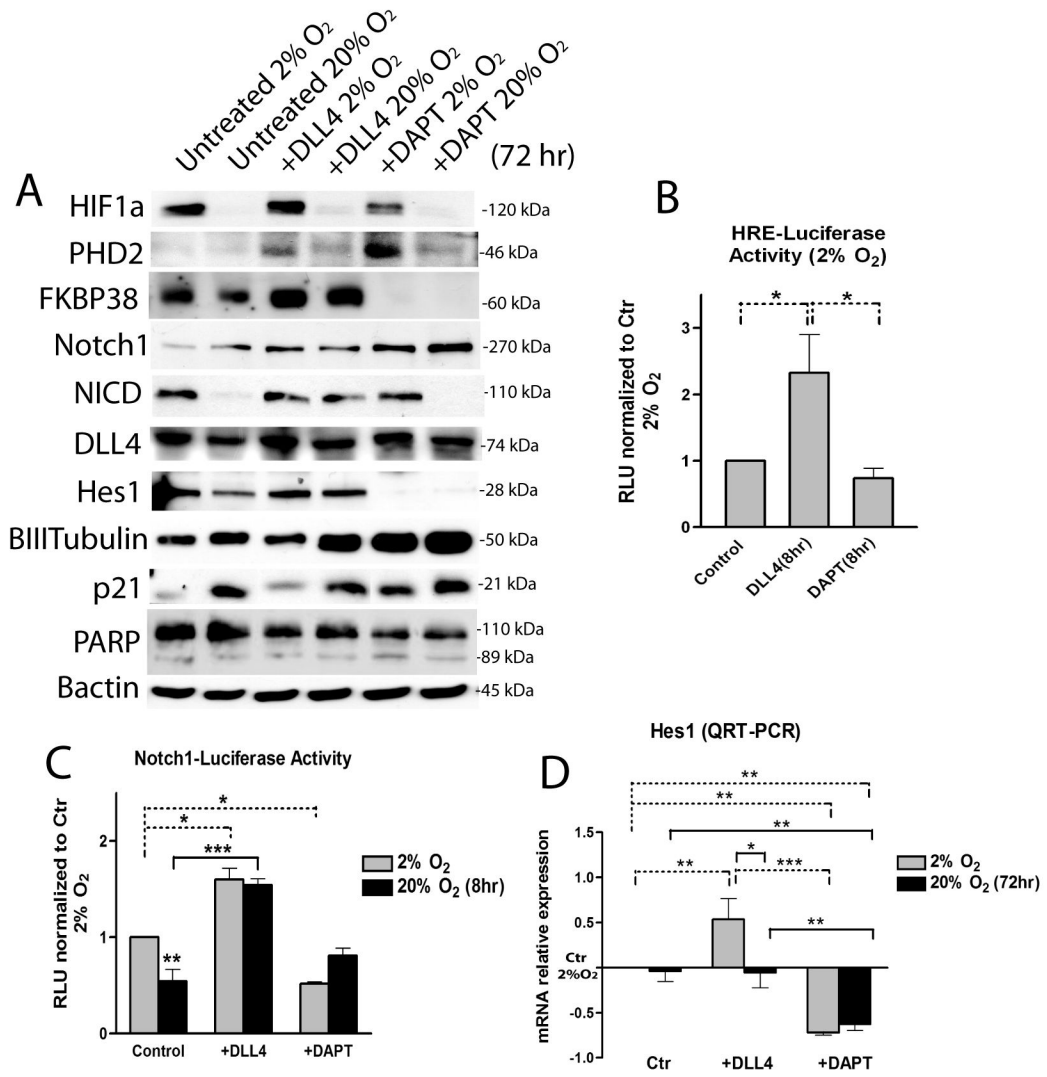


**Figure 5. Effects of Notch1 signaling exogenous modulation by Dll4 and DAPT on MDB cells** (A) Representative western blot analyses of HIF-1 $\alpha$ , PHD2, FKBP38, Notch1, NICD, Dll4, Hes1,  $\beta$ -III-tubulin, p21<sup>cip1</sup>, PARP and  $\beta$ -actin of MDB derived cells cultured for 72 hrs in presence of either immobilized Dll4 (2  $\mu$ g/ml) or DAPT (10  $\mu$ M) at either 2% or 20% oxygen. (B) HRE-luciferase transfected cells in the same conditions as in (A) at 2% oxygen. (C) Notch1-luciferase transfected MDB cells treated with Dll4 and DAPT for 8 hr as described in Materials and Methods. For both B and C, values are expressed in RLU (= relative light units). (D) QRT-PCR analysis of *hes1* normalized to *gusb* and then calibrated to 2% oxygen control. Mean  $\pm$  S.E.M of 3 different MDB. \*p < 0.05, \*\*p < 0.01, \*\*\*p < 0.001.

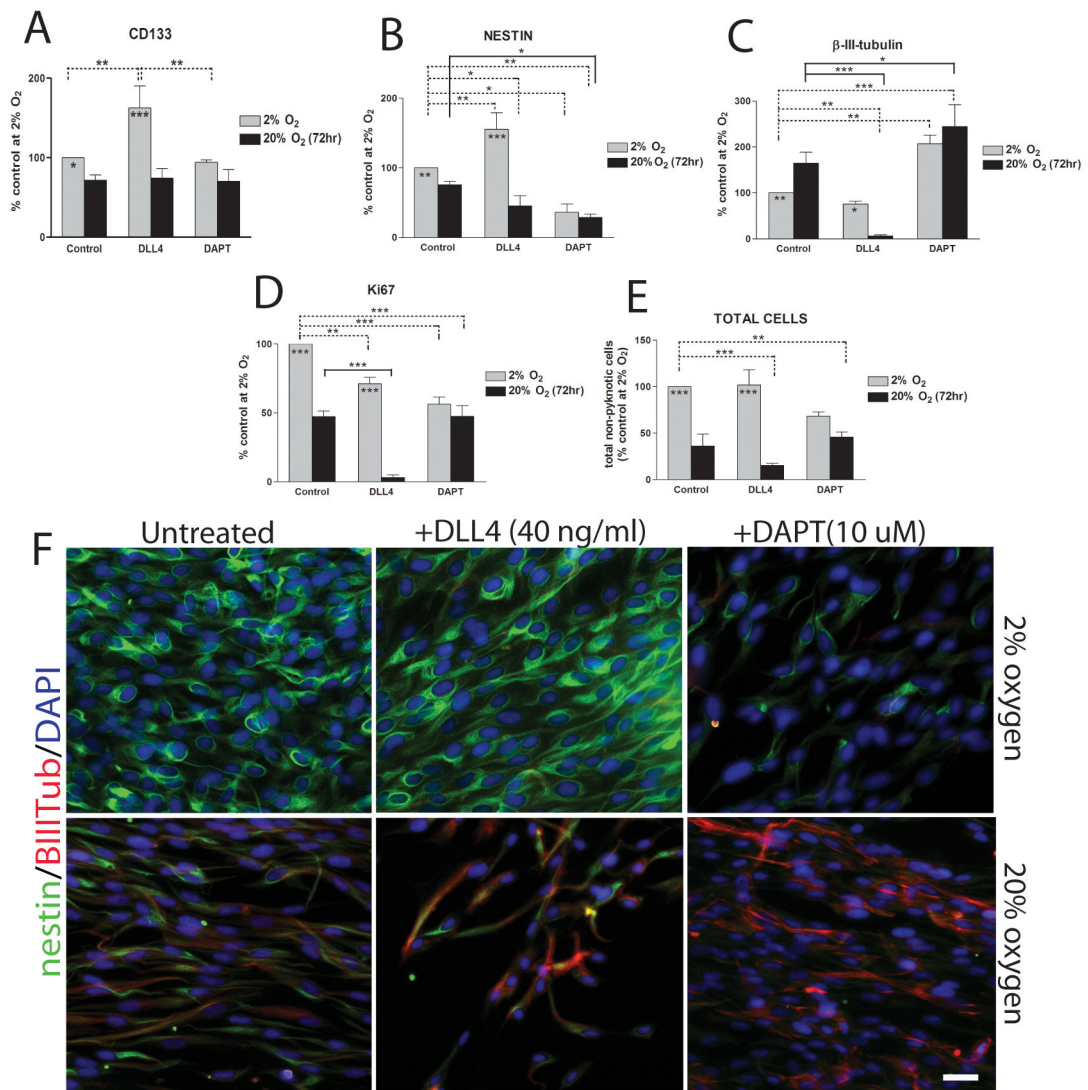


**Figure 6. Notch1 signaling modulation by Dll4 and DAPT affects MDB cell phenotype depending on hypoxia**

(A) Percentages of CD133<sup>+</sup> cells of MDB derived cells cultured for 72 hr in presence of either immobilized Dll4 (2 μg/ml) or DAPT (10 μM) at either 2% or 20% oxygen. Mean of 3 tumors ± S.E.M., n = 2 for each tumor. (B-E) Immunocytochemical analysis for nestin (B) β-III-tubulin (C), Ki67 (D) and total cell quantification relative to total DAPI<sup>+</sup> cells (E). MDB cells were treated as described in (A). Mean of 6 tumors ± S.E.M. (F) Representative immunocytochemical images of nestin (green)/β-III-tubulin (red) staining. 20X pictures, bar = 40 μm. \*p < 0.05, \*\*p < 0.01, \*\*\*p < 0.001.

**Table 1**Phenotypic identity of HIF-1 $\alpha$ <sup>+</sup> and HIF-1 $\alpha$ <sup>-</sup> MDB cells

HIF-1 $\alpha$ status	Nestin	$\beta$ -III-tubulin	CD133	Notch1	Hes-1
HIF-1 $\alpha$ <sup>+</sup>	57.92 $\pm$ 6.35	2.33 $\pm$ 1.2	46.88 $\pm$ 5.97	78.57 $\pm$ 7.05	84.7 $\pm$ 7.06
HIF-1 $\alpha$ <sup>-</sup>	4.2 $\pm$ 1.59	63.33 $\pm$ 4.35	5.57 $\pm$ 1.02	8.86 $\pm$ 4	8.71 $\pm$ 3.71

Values represents mean of 5 different MDB samples  $\pm$  SEM. Data are expressed as percentages of total DAPI<sup>+</sup> cells.